Determining the Plio-Quaternary uplift of the southern French massif-Central; a new insights for intraplate orogen dynamics.

Oswald Malcles[1], Philippe Vernant[1], Jean Chéry[1], Pierre Camps[1], Gaël Cazes[2,3], Jean-François Ritz[1], David Fink[3].

[1] Geosciences Montpellier, CNRS-University of Montpellier, Montpellier, France

[2] SEES, University of Wollongong, Wollongong, Australia

[3] Australian Nuclear Science and Technology Organisation, Lucas Heights, Australia

Correspondence to: Oswald Malcles (oswald.malcles@umontpellier.fr)

Abstract.

The evolution of intra-plate orogens is still poorly understood. Yet, this is of major importance for understanding the Earth and plate dynamic, as well as the link between surface and deep geodynamic processes. The French Massif Central is an intraplate orogen with a mean elevation of 1000m, with the highest peak elevations ranging from 1500m to 1885m. However, active deformation of the region is still debated due to scarce evidence either from geomorphological or geophysical (i.e. geodesy and seismology) data. Because the Cévennes margin allows the use of karst sediments geochronology and morphometrical analysis, we study the vertical displacements in that region: the southern part of the French Massif-Central. Geochronology and morphometrical results, helped with lithospheric-scale numerical modelling, allow, then, a better understanding of this intraplate-orogen evolution and dynamic.

Using the ability of the karst to durably record morphological evolution, we first quantify the incision rates. We then investigate tilting of geomorphological benchmarks by means of a high-resolution DEM. We finally use the newly quantified incision rates to constrain numerical models and compare the results with the geomorphometric study.

We show that absolute burial age ($^{10}Be/^{26}Al$ on quartz cobbles) and the paleomagnetic analysis of karstic clay deposits for multiple cave system over a large elevation range correlate consistently. This correlation indicates a regional incision rate of 83 $^{+17}/_{-5}$ $m.Ma^{-1}$ during the last ca 4 Myrs (Plio-Quaternary). Moreover, we point out through the analysis of 55 morphological benchmarks that the studied region has undergone a regional southward tilting. This tilting is expected as being due to a differential vertical motion between the north and southern part of the studied area.

Numerical models show that erosion-induced isostatic rebound can explain up to two-thirds of the regional uplift deduced from dating technics and are consistent with the southward tilting obtain from morphological analysis. We presume that the remaining part is related to dynamic topography or thermal isostasy due to the Massif Central plio-quaternary magmatism.

1 Introduction and Tectonic Setting

1.1 Introduction

Since the past few decades, plate-boundary dynamics is to a first order, well understood. Such is not the case for intraplate regions, where short-term (10^3-10^5 yrs.) strain rates are low and the underlying dynamical processes are still in debate (e.g. Calais et al., 2010; Vernant et al., 2013; Calais et al., 2016; Tarayoun et al., 2017). On geological time-scales, transient phenomenon that are classically used to explain intraplate deformations (as seen through the seismic activity) can not be a satisfactory explanation though, this then raises the question of the origin of the high finite deformations observed in many parts of the world as for instance the Ural mountains in Russia, the Blue Mountains in Australia or the French Massif Central.

In this study we focus on the Cevennes Mountains and the Grands Causses regions that form the southern part of the French Massif Central, located in the southwestern Eurasian plate (fig.1). The region is characterized by a mean elevation of 1000 m with summits higher than 1500 m. Such topography is likely to be the result of recent, active uplift and as the Cevennes mountains experiences an exceptionally high mean annual rainfall (the highest peak, Mount Aigoual, records the highest mean annual rainfall in France of 4015 mm) it raises the question of a possible link between erosion and uplift as previously proposed for the Alps (Champagnac et al., 2007; Vernant et al., 2013; Nocquet et al., 2016). This region currently undergoes a small but discernible deformation, but no significant quantification can be deduced due to the scarcity in seismicity (Manchuel et al., 2018). In addition, GPS velocities are below the uncertainty threshold of GPS analyses (Nocquet et Calais, 2003; Nguyen et al., 2016).

South and West of the crystalline Cevennes mountains, prominent limestone plateaus, named Grands Causses rise to 1000m and are dissected by few canyons that are several hundreds of meter deep (Topographic font in figure 1 show first order topography and morphology). The initiation of incision, its duration and the geomorphic processes leading to the present-day landscape remain poorly constrained. A better understanding of the processes responsible for this singular landscape would bring valuable information on intraplate dynamics, especially where large relief exists.

The oldest formations in the area were formed during the Variscan orogeny (late Palaeozoic, ~300 Ma; Brichau et al., 2007) and constitute the crystalline basement of the Cevennes. Between 200 and 40 Ma (Mesozoic and lower Cenozoic), the region was mainly covered by the sea ensuring the development of an important detrital and carbonate sedimentary cover, which can reach several km thick in some locations (Sanchis and Séranne, 2000; Barbarand et al., 2001). During the Mesozoic era, an episode of regional uplift and subsequent erosion and alteration (called the Durancian event) is proposed as being at the origin of the flat, highly elevated surface that persists today across the landscape (Bruxelles, 2001; Husson, 2014).

The area is also affected by the major NE-SW trending Cevennes fault system. During the Pyrenean orogeny, 85 to 25 Ma (Tricart, 1984; Sibuet et al., 2004), several faults and folds affected the geological formations south of the Cevennes fault, while very few deformation occurred further north within the Cévennes and Grand Causses areas (Arthaud and Laurent, 1995). Eventually, the Oligocene extension (~30 Ma) led to the counterclockwise rotation of the Corso-Sardinian block and the opening of the Gulf of Lion, re-activating some of the older compressive structures as normal faults. The main drainage divide between the Atlantic Ocean and the Mediterranean Sea is located in our study area and is inherited from this extensional episode (Séranne et al., 1995; Sanchis et al., 2000).

Superimposed at the inheritance from Durancian event, the last two major tectonic episodes which are the Pyrenean compression and the Oligocene extensionshaped the large-scale structural morphology of the region. Afterwards during the Plio-Quaternary period, only intense volcanic activity has affected the region, from the Massif Central to the Mediterranean shoreline. This activity is characterised by several volcanic events that are well constrained in age (Dautria et al., 2010). The last eruption occurred in the Chaîne des Puys during the Holocene (i.e. the past 10 kyrs (Nehlig et al., 2003; Miallier et al., 2004). Some authors proposed that this activity is related to a hotspot underneath the Massif Central (Granet et al., 1995; Baruol and Granet, 2002) leading to an observed positive heat-flow anomaly and a possible regional plio-Quaternary uplift.

Despite this well described overall geological evolution the onset of active incision that has shaped the deep valleys and canyons (e.g. Tarn or Vis river, Fig 1) across the plateaus, and the mechanisms that controlled this incision are still in debate. One hypothesis proposes that canyon formation was driven by the Messinian salinity crisis with a drop of more than 1000m in Mediterranean Sea level. This, however, would then not explain the fact that the Atlantic watersheds show similar incision. Other studies suggested that the incision is controlled by the collapse of cave galleries that lead to fast canyon formation mostly during the late Quaternary, thus placing the onset of canyon formation only a few hundreds of thousands of years ago (Corbel, 1954). In contrast, it has also been proposed more recently (based on relative dating techniques and sedimentary evidence) that incision during the Quaternary was negligible (i.e. less than a few tens of meters), and that the regional morphological structures seen today occurred around 10 Ma (Séranne et al., 2002; Camus, 2003).

1.2 Working hypothesis

In this paper, we provide new quantitative constraints on both the timing of incision and the rate of river down-cutting in the central part of the Cévennes and of the Grands Causses that has resulted in the large relief between plateau and channel bed. We employ two methods, cosmogenic $^{10}Be/^{26}Al$ burial dating of quartz cobbles that have been transported by rivers and paleomagnetic analyses along vertical profiles of endokarstic clay both of which have been deposited in multiple cave systems at the time cave entry was at river channel elevation. In parallel, by analysing a high-resolution DEM (5m), we show that the region is affected by a regional tilting. Our results allow to quantify the role of the Plio-Quaternary incision on the Cévennes landscape evolution and to constrain numerical modelling from which we derive the regional uplift rates and a tilt of geomorphological markers.

One important point of this study is the integration of multi-disciplinary approaches in order to constrain intraplate deformation. Such an approach is necessary to bring new insights into the lithosphere behaviour of slow dynamic regions. If the uplift is easily recognisable in the landscape (1000 m high plateaus), quantifying its timing and evolution rates is harder and can't be performed by classical technics (e.g. GPS). This is why we aim to quantify the incision rate over the longest possible period thanks to the karstic immunity. Dealing with long-term incision rates (up to 5 Myrs) should permit to smooth possible climatic-driven incision rate variations (with time-span of several kyrs).

If incision is initiated by uplift centred on the North of the area where elevations are maximum, it will lead to tilting of fossilised topographic markers as strath terraces. Our method of analyses provides an opportunity to select between three possible explanations for the current terrain morphology. The first is based on old uplift and old incision (Fig. 2.A). In this case, apparent incision rates would be very low. For instance, if incision commenced 10 Ma (Serrane et al., 2002), we would find surface tilting but cosmogenic burial dating with $^{10}Be/^{26}Al$ which cannot discern ages older than ~ 5Ma due to excessive decay of 26Al, would not be possible. The second possibility (Fig. 2.B) is that the uplift is old, and incision consequently follows but with a time lag. Here the incision rate would be rather fast but no tilting is expected for the river-related markers because no differential uplift occurs after their formation. Finally, the third possibility (Fig 2.C) is that uplift and incision are concurrent and recent (i.e. within the time scale of cosmogenic burial dating) and thus we would expect burial ages < 5 Myrs relatively high incision rates, and tilting of morphological markers. These different proposals for the temporal evolution of the region will then be compared using numerical modelling.

2. Determining the incision rates in the Cévennes and the Grand Causses Region

2.1. Principles and methods

2.1.1. Karst model

No evidence of important aggradation events has been reported in the literature for the studied area. Therefore we base our analysis on a per descensum infill model of the karst networks whereby sediments are transported and then deposited within cave galleries close to base level. When cave-systems and entry passages are near the contemporaneous river channel elevation (including higher levels during floods), the deposition into caves of sediments, from clay to cobbles occurs, especially during flood events. Subsequent river incision into bedrock creates a relative base level drop (due to uplift or sea-level variations). The galleries associated with the former base-level are now elevated above the new river course and become disconnected from further deposition. Hence fossilised and trapped sediments throughout the cave network represent the cumulative result of incision. In this commonly used model (Granger et al., 1997; Audra et al., 2001; Stock et al., 2005; Harmand et al., 2017), the higher the gallery elevation (relative to the present-day base level) the older the deposits in that gallery. As a result, the objective here is to quantify a relative lowering of the base level in the karst systems, with the sediments closest to the base level being the youngest deposits, and note that we do not date the cave network creation which may very well pre-date river sediment deposition.

Within individual canyons, successions of gallery networks across the full elevation range from plateau top to modern river channel, were not always present and often sampling could not be conducted in a single vertical transect. Thus we make the assumption of lateral altitudinal continuity i.e. that within a watershed, which may contain a number of canyons, the sediments found in galleries at the same elevation were deposited at the same time. Inside one gallery, we use the classical principle of stratigraphy sequence (i.e. the older deposits are below the younger ones). More informations and detailed relationship concerning the karstic development and geometric relationship between karstic network and morphological markers could be find in Camus (2003). In any cases, our aim is not to date the galleries formation, neither to explain the formation processes (e.g. past preferential alteration layer); but to use the time information brought by the sediment that have been trapped into the cave system. Therefore, we apply the common used model (example in Harmand et al., 2017) that had been proved by Granger et al., (1997, 2001). For cave topographic survey, we refer the reader to https://data.oreme.org/karst3d/karst3d_map providing 3D survey.

2.1.2. Burial ages

Burial dating using Terrestrial cosmogenic nuclides (TCN) is nowadays a common tool to quantify incision rates in karstic environment (Granger and Muzikar, 2001; Stock et al., 2005; Moccochain., 2007; Tassy et al., 2013; Granger et al., 2015; Calvet et al., 2015; Genti, 2015; Olivetti et al., 2016; Harmand et al., 2017; Rovey II et al., 2017; Rolland et al., 2017; Sartégou, 2017; Sartégou et al., 2018). This method relies on the differential decay of TCN in detrital rocks that were previously exposed to cosmic radiation before being trapped in the cave system. With this in mind, the ^{10}Be and ^{26}Al nuclide pair is classically used as (i) both nuclides are produced in the same mineral (i.e. quartz), (ii) their relative production ratio is relatively well constrained (we use here a standard ^{26}Al/^{10}Be pre-burial ratio of 6.75, see Balco et al., 2008) and (iii) their respective half-lives (about 1.39 Myr and 0.70 Myr for ^{10}Be and ^{26}Al, respectively) are well suited to karstic and landscape evolution study, with a useful time range of ~100 ky to ~5 Myr.

To quantify the incision rate of the limestone plateau of the Cevennes area, we analysed quartz cobbles infilling from four caves of the Rieutord canyon (Fig. 1), this canyon is well suited for such study because horizontal cave levels are tiers over 200 m above the current river-level and are directly connected to the canyon, leading to a straight relationship between river elevation and the four cave infilling that we have sampled (Cuillère cave, Route cave, Camp-de-Guerre cave and Dugou cave). Furthermore, cobbles source is well known and identified: the upstream part of the Rieutord river, some tens of kilometres northward, providing a unique sediment origin composed of granite and metamorphic rocks embedding numerous quartz veins.. All samples (Example Fig. 3) were collected far enough away (>20m) from the cave entrance and deep enough below the surface (>30m) to avoid secondary in-situ cosmogenic production of ^{10}Be and ^{26}Al in the buried sediments.

The quartz cobbles were first crushed and purified for their quartz fraction by means of sequential acid attack with Aqua-Regia (HNO_3 +3HCl) and diluted Hydrofluoric acid (HF). Samples were then prepared according to ANSTO's protocol (see Child et al. 2000) and ~300µg of a ^{9}Be carrier solution was added to the purified quartz powder before total dissolution. AMS measurements were performed on the 6MV SIRIUS AMS instrument at ANSTO and results were normalised to KN-5-2 (for Be, see Nishiizumi et al., 2007) and KN-4-2 (for Al) standards. Uncertainties for the final ^{10}Be and ^{26}Al concentrations include AMS statistics, 2% (Be) and 3% (Al) standard reproducibility, 1% uncertainty in the Be carrier solution concentration and 4% uncertainty in the natural Al measurement made by ICP-OES, in quadrature. Sample-specific details and results are found in table 1.

2.1.3. Paleomagnetic analysis

In parallel with burial dating, we analyzed the paleomagnetic polarities within endokarstic clay deposits within two main cave systems: the *Grotte-Exsurgence du Garrel* and the *Aven de la Leicasse* (Fig. 1). These two cave systems allowed us collecting samples along a more continuous range of elevations than the one provided by the Rieutord samples (for burial age determination) and also extending the spatial coverage to the Southern Grands Causses region. Thanks to the geometry of these two cave systems, we sampled a 400m downward base level variation. The sampling was done along vertical profiles from a few ten of centimeters to 2 meters high by means of Plexiglas cubes with a 2 cm edge length (Fig. 4) used as a pastry cutter. We weren't able to analyse clay samples from Rieutord canyon because no reliable clay infilling was found in the Rieutord caves.

Demagnetisation was performed with an applied alternative field up to 150mT using a 2G-760 cryogenic magnetometer, equipped with the 2G-600 degausser system controller. Before this analysis, each sample remained at least 48h in a null magnetic field, preventing a possible low coercivity viscosity overprinting the detrital remanent magnetisation (DRM) (Hill, 1999; Stock et al., 2005; Hajna et al., 2010). If the hypothesis of instantaneous locked in DRM seems reasonable compared with the studied time span, it is important to keep in mind that the details of DRM processes (as for instance the locked in time) is not well understood (Tauxe et al., 2006; Spassov et Valet, 2012) and could possibly lead to small variations (few percents) in the following computed incision rates.

Because fine clay particles are expected being easily reworked in the cave, careful attention was paid to the site selection and current active galleries were avoided. Clays deposits had to show well laminated and horizontal layering in order to prevent analysis of in-situ produced clays (from decalcification) or downward drainage by an underneath diversion gallery that could strongly affect the obtained inclination (and also the declination to a minor extent). Note that for paleo-polarities study alone, small inclination or declination variations won't result in false polarities

2.2 Quantifying the average incision rates

2.2.1. Rieutord incision rate from burial ages

The relationship between burial ages and incision is shown in Figure 5. For the four caves, we observed a good relationship between burial ages and finite incision, except for the Camp-de-Guerre cave (CDG) site, the higher the cave is, the older the burial ages are. Burial ages for the Cuillère cave, Dugou cave, Camp-de-Guerre cave and Route cave are 2.16 ± 0.15, 0.95 ± 0.14, 0.63 ± 0.1 and 0.21 ± 0.1 Myrs respectively. This is consistent with the supposed cave evolution and first-order constant incision of the Rieutord canyon. CDG age has to be considered with caution. The CDG cave entrance located in a usually dry thalweg can act as a sinkhole or an overflowing spring depending on the intensity of the rainfall. The sample was collected in a gallery showing evidence of active flooding ~10 m above the Rieutord riverbed, therefore the older than expected age, given the elevation of the cave, is probably due to cobbles that came from upper galleries during flood events. Forcing the linear regression to go through the origin, leads to an incision rate of 83 ± 35 $m.Ma^{-1}$. These results show that at least half of the 300 m deep Rieutord Canyon is a Quaternary incision. Extrapolating the obtained rate yields an age of 4.4 ± 1.9 Ma for the beginning of the canyon incision, which suggests that the current landscape has been shaped during the Plio-Quartenary period. To extend our spatial coverage and bring stronger confidence into our results, we combine Rieutord burial ages with paleomagnetic data from watersheds located on the other side of the Herault watershed.

2.2.2. South Grands Causses incision rate from paleomagnetic data

A total of 100 clay-infilling samples distributed over of 13 sites (i.e. profiles) were studied. The lowest sample elevation above sea level (a.s.l.) is in the Garrel (ca 190 m) and the highest in the Leicasse (ca 580 m a.s.l.). In the Leicasse cave system, we sampled 8 profiles totalizing 60 samples. Profiles elevations are located between ca 200 m and ca 400 m above the base level (a.b.l.), which corresponds to the elevation of the Buèges river spring at 170 m a.s.l.

In the Garrel cave system, we sampled 5 profiles totalizing 40 samples that range between 20 m and 80 m a.b.l. defined by the Garrel spring at 180 m a.s.l. Given the very marginal difference in elevation between the local base levels from these two caves, we assume that they have the same local base level. At each studied sites, if all the profile samples have the same polarity, the site is granted with the same polarity, either normal or reverse. If not (i.e. the profile displays normal and reverse polarities), we consider it as a transitional site. Figure 6 shows the results plotted with respect to the paleomagnetic scale (x axis) for the past 7 Ma, and their elevation above the base level (y axis). The measured paleomagnetic polarities on each sites is plotted several times for given incision rates supposed to be constant through times (this allows determining different age models and analyze their correlation with the distribution of paleomagnetic data, see below).First, we note a good agreement between samples located at the same elevation elevation and being part of the same stratigraphic layer (Camus, 2003). This syngenetic deposition allow, as best explanation to prevent from a possible partial endokarstic reworking. Second, the different elevations of the galleries where we collected the samples allow proposing that the Leicasse deposits encompass at least three chrons, while the Garrel deposits encompass only one. Third, a transitional signal comprised between a reversal signal (lower samples) and a normal signal (upper ones) is observed at Les Gours sur Pattes (LGP) sampling site (Fig. 7). This provides a strong constraint on the age of the sediment emplacement in the Leicasse with respect to the magnetostratigraphic timescale (Fig. 6).

Compared to the Leicasse cave system, the elevation/polarity results for the Garrel are less constrained. Only one site shows a reverse polarity at 90 m a.b.l., and the transitional polarity found at 40 m a.b.l. is unclear (tab, suppl mat.). The rest of the polarities (72 samples) are all normal. Given that a U-Th ages younger than 90 kyrs was obtained for two speleothems (Camus, 2003) covering our samples collected at 40 m a.b.l. (Fig. 6), we consider that the emplacement of the clays deposits occurred during the most recent normal period and are therefore younger than 0.78 Ma (Figure 6). The transition between the highest normal sample and the reversed one is located somewhere between 78 m and 93 m a.b.l. suggesting a maximum base level lowering rate of 109 ± 9 m.Ma^{-1}.

To go further in the interpretation of our data, and better constraint the incision rate, we performed a correlation analysis between observed and modelled polarities for a 0 - 200 m.Ma-1 incision-rate range (linear rate, each 1m.Ma-1). Modelled polarities are found using the intersection between sample elevation and incision-rate line. We obtained 10 possible incision rates with the same best correlation factor (Fig. 8) spanning from 43 to 111 m.Ma^{-1} (mean of 87 ± 24 m.Ma^{-1}). Taking into account the transitional signal of the LGP site in the Leicasse cave yields a linear incision rate of 83 $^{+17}/_{-5}$ m.Ma^{-1}. Proposed uncertainties are based on previous and next transition-related estimated incision rate.

Using a similar approach for the Rieutord crystalline samples, that is to say we compute, for the same incision-rate space, the distance in a least square sens between the modeled age and the measured ones in order to check the cost function shape and acuteness. With this method, we determined a linear incision rate of 85 ± 11 m.Ma^{-1} (Fig 8). Those two results, based on independent computations, suggest the same first-order incision rate for the last 4 Ma of 84 $^{+21}/_{-12}$ m.Ma^{-1}. Given that the Rieutord, Garrel and Buèges rivers are all tributaries of the Hérault river, we propose that this rate represents the incision rate for the Hérault river watershed, inducing approximately 300-350 m of finite incision over the Plio-Quaternary period.

If the landscape is at first order in an equilibrium state, that is to say, if we preclude our incision rates being a regressive erosional signal, the incision needs to be balanced by an equivalent amount of uplift. If the uplift rate is roughly correlated to the regional topography, lowest uplift rates would be expected in the south of our sampling sites inducing regional tilting of morphological benchmarks. In the next part, we search for such evidences that would suggest differential uplift.

2.3 Geomorphometrical approach

According to the Massif-Central centered uplift hypothesis, morphological markers such as strath terraces, fluvio-karstic surfaces or abandoned meanders should display a southward tilting due to differential uplift between the northern and the southern part of the region.

To investigate these different signals, we used the morphological markers available for the study area (Fig. 9). We used a 5 m resolution DEM analysis to identify the markers corresponding to surfaces with slope < 2°. This cut-off slope angle prevents to identify surface related to local deformation such as for example landslide or sinkhole. Other issue could be due to diffusion processes that could create apparent tilting. However that problem is adress by 1) the automatic selection and correction and the final manual check for residue random distribution (see below).The local river slope is on the order of 0.1° so the 2° cut-off angle is far from precluding to identify tilted markers. We also us a criterion based on an altitudinal range for a surface. This altitudinal span is set individually for each surface based on elevation, slope and curves map analysis, and encompass from few meters to tens of meters depending on the size of the marker. We checked 80% of the identified surfaces in the field in order to avoid misinterpretation. Some pictures are provided in supplementary material. The dip direction and angle of the surface in computed in a two steps approach. First, we fit a plan using extracted points from the DEM inside the delimited surface. Second, based on this plan we remove the DEM points with residuals 3 times larger than the standard error and compute more accurate plan parameters (second fitting). This outlier suppression removes any inaccurate DEM points and correct for inaccurate surface delimitation (e.g. integration of a part of the edge of a strath terrace, diffusion processes marks, etc.).

Because no obvious initially horizontal markers are known, we propose to correct the marker current slope by the initial one to quantify the tilt since the marker emplacement. To do so we follow the method used by Champagnac et al. (2008) for the Forealps. We identify the drain related to the marker formation and compute its current local slope and direction. This method assumes that landscapes are at the equilibrium state and that the river slope remained constant since the marker formation. This assumption seems reasonable given the major river profiles and because most of the markers used are far from the watershed high altitude areas precluding a recessive erosional signal. Finally, we removed the local river plan from the DEM extracted surface.

Following this methodology, we obtained 61 surfaces. We then applied three quality criterions to ensure the robustness of our results: 1) The minimal surface considered is 2500 m^2 based on a comparison between the 5m resolution DEM and a RTK GPS survey over 3 strath terraces (Hérault river); 2) Final plans with dip angles larger than 2° are removed; 3) The residuals for each geomorphological marker must be randomly distributed without marker edge signal, or clear secondary structuration. Only 38 markers meet those 3 quality criterions.

If the identified and corrected markers had indeed registered an differential uplift between the north and the south, we expected the following signals:

- The dipping direction of the tilted markers should be parallel to the main gradient of the topography, i.e. between 150°E and 180°E for our studied region. This expectation is the most important one, regarding uncertainties on the uplift rate and lithospheric elastic parameters.

- A latitudinal tilting trend, i.e. an increase of the tilt angle along the topography gradient. Indeed, null or small tilts are expected near the shoreline and within the maximum uplift area of the Cevennes/Massif Central, while the maximum tilt is expected at a mid-distance between these two regions, i.e. about 50 km inland from the shoreline.

- A positive altitudinal tilting trend (an increase in dip angle with altitude). This trend would be representative of the accumulation of finite tilt. However, it supposes a linear relationship between the altitude and the age of the marker formation. If at first order, this straightforward hypothesis seems reasonable for river-controlled markers (e.g. strath terraces), other surfaces are hardly expected to follow such an easy relationship.

Among the three expected signal, southward dipping is robustly recorded with a mean tilt angle of 0.60 ± 0.40 ° with an azimuth of N128 ± 36°E (Fig. 10). Latitudinal trend and altitudinal trend are less robustly reached but that is not surprising because of the strong susceptibility to local phenomenon or even so lack of robust age constraint.

3 Numerical modelling

Both geomorphological and geochronological evidence suggest a Plio-Quaternary uplift of the Cevennes area. The origin of such uplift could be associated with several processes: erosion-induced isostatic rebound, dynamic topography due to mantle convection, thermal isostasy, residual flexural response due to the Gulf of Lion formation, etc. For the Alps and Pyrenees mountains, isostatic adjustment due to erosion and glacial unloading has been recently quantified (Champagnac et al., 2007, Vernant et al., 2013; Genti et al, 2016, Chery et al. 2016). Because the erosion rates measured in the Cevennes are similar to those of the Eastern Pyrenees (Calvet et al., 2015, Sartégou et al., 2018a), we investigate by numerical modelling how an erosion-induced isostatic rebound could impact the southern Massif Central morphology and deformation.

We define a representative cross-section parallel to the main topographic gradient (i.e. NNW-SSE) and close to the field investigation areas (Figure 11). We study the lithospheric elastic response to erosion with the 2D finite element model ADELI (Hassani et Chery, 1996; Chéry et al. 2016). The model is composed of a plate accounting for the elasticity of both crust and uppermost mantle. Although the lithosphere rigidity of the European plate in southern Massif central is not precisely known, vertical gradient temperatures provided by borehole measurements are consistent with heat flow values ranging from 60 to 70 $mW.m^2$ (Lucazeau et Vasseur, 1989). Therefore, we investigate plate thickness ranging from 10 to 50 km as done by Stewart et Watts (1997) for studying the vertical motion of the alpine forelands. We choose values for Young's and Poisson parameters of respectively 10^{11} Pa and 0.25, both commonly used values for lithospheric modelling (e.g. Kooi et Cloething, 1992; Champagnac et al. 2007, Chéry et al., 2001). This leads to long-term rigidity of the lithosphere model ranging from 10^{21} to 10^{25} N.m. Since the effect of mantle viscosity on elastic rebound is assumed to be negligible at the time scale of our models (1 to 2 Myrs), we neglect the visco-elastic behaviour of the mantle. Therefore, the base of the model is supported by an hydrostatic pressure boundary condition balancing the weight of the lithosphere (Fig. 11). Horizontal displacements on vertical sides are set to zero since geodetic measurements show no significant displacements (Nocquet et Calais, 2003; Nguyen et al., 2016). The main parameters controlling our model are the erosion (or sedimentation) triggering isostatic rebound and the elastic thickness. The erosion profile (Fig. 11) is based on topography, our newly proposed incision rate and other studies (Olivetti et al., 2016 for onshore denudation and Lofi et al., 2003; Leroux et al., 2014 for offshore sedimentation). This profile is a simplification of the one that can be expected from Olivetti et al. (2006) and do not aim at matching precisely the published data because of, first, the explored time-span (~ 1 Myrs) is not covered by thermochronological data (> 10Myrs) or cosmogenic denudation rate (10s-100s kyrs). Second, we base our erosion rate as being linked with local (10s km^2) slopes, that are higher near the drainage divide. We, by this aim can invoke any kind of erosion processes (e.g. landslides). Third, the model suppose a cylindrical structure and then, high-frequency lateral variations in term or actual denudation rate or proxy (slope, elevation, etc.) must be averaged. Concerning this erosion profile, parametric study (highest erosion rate ranging from 1 to 1000 $m.Myrs^{-1}$) give no difference in the interpretation and, for few percent variations, only few percent variations in the modeled uplift-rate.

The flexural rigidity controls the intensity and wavelength of the flexural response and ranges from 10^{21} to 10^{25} N.m. It can be expressed as a variation in elastic thickness (Te) ranging from 4.4 to 96 km (Fig. 12). We also test a possible Te variation between inland and offshore areas. For the following discussion, we use an elastic thickness of 15km corresponding to a value of D of 3.75 $x10^{23}$ $N.m^{-1}$. In this case, the inland and offshore parts are largely decoupled and the large sedimentation rate in the Gulf of Lion does not induce a flexural response on the Cévennes and Grands Causses areas. With a maximum erosion rate of 80 $m.Ma^{-1}$ (Fig 11), the models display uplift rates of 50 $m.Ma^{-1}$ over more than 100 km. As previously explained, the finite incision is permitted by an equal amount of uplift considering that the incision is not due to regressive erosion. If all tested models show uplift, the modelled amplitudes are smaller than the expected ones. To obtain the same uplift rate than the incision rates, the applied erosion rate over the model must be increased. However, we assume that the landscape is at equilibrium, so, if the erosion rate is increased, it will be higher than the incision rate leading to the decay of relief over the area. No evidence of such evolution is found over the region and, if further studies need to be done to quantify the actual erosion rate, we mostly think that a second process is acting, inducing the rest of the uplift that can't be obtained by the erosion–induced isostatic adjustment. Finally, models predict a seaward tilt of the surface at the regional-scale (Fig. 13), in agreement with the observed tilting of morphological markers.

4. Discussion

We assume that the sediments collected in the karst were deposited per descensum, i.e. we do not know if the galleries existed a long time before or were formed just before the emplacement of the sediments, but the more elevated the sediments are, the older their deposit is. If there is no evidence of an important aggradation episode leading to more a complex evolution as proposed for the Ardèche canyon (Moccochain et al., 2007; Tassy et al., 2013), we point out that small aggradation or null erosion period could, however, be possible. Some processes could explain such relative stability: e.g. variation in erosion (due to climatic fluctuation) or impact of eustatic variations (in river profile, flexural response, etc.). Such transient variations have been shown for the Alps (Saillard et al., 2014; Rolland et al., 2017) and are proposed as being related to climato-eustatic variations and therefore should last 10 to 100 kyrs at most.

Based on our sampling resolution, we cannot evidence such transient periods and we must use an average base level lowering rate in the karst, which we correlate to the incision of the main rivers. The TCN-based incision rate derived from the Rieutord samples (83 ± 35 m.Ma^{-1}) is consistent with the one derived from the Garrel (U-Th ages: 85.83 m.Ma^{-1} according to the sole U/Th exploitable result (Camus, 2003)) and from the Garrel-Leicasse combination (Paleomagnetic approach: 84 $^{+21}/_{-12}$m.Ma^{-1}).

This mean incision rate of ca. 85 m.Ma^{-1} lasting at least 4 Ma, highlights the importance of the Plio-Quaternary period into the Cévennes and Grand Causses morphogenesis. Furthermore, the 300 to 400 m of incision precludes a relative base level controlled by a sea-level drop. Indeed, documented sea level variations are less than 100 m (Haq, 1988, Miller et al., 2005). Furthermore, the Herault river does not show any significant knickpoints or evidence of unsteadiness in its profile as expected if the incision was due to eustatic variations. Therefore, we propose that the incision rate of ~85 m.Ma^{-1} is due to a plio-quaternary uplift of the Cévennes and Grands Causses region.

Other river-valley processes could lead to a local apparent high incision rate as for instance major landslide or alluvial fan (Ouimet et al., 2008). This hypothesis of an epigenetic formation of the Rieutord is irrelevant because of i) none of the possible causes had been found in the Rieutord canyon and ii) the consistency of the TCN-based incision rate and the paleomagnetic-based incision rate for two other cave-systems. Indeed, the use of two independent approaches and three locations is a good argument in favour of the robustness of our proposed mean 85 m.Ma^{-1} incision rate. Yet, using more data, particularly burial dating colocalized with clays samples and adding sampling sites would give a stronger statistical validation. In the Lodève basin (Point 4, fig. 1), inverted reliefs allow another independent way to quantify minimal incision rate. K/Ar and paleomagnetic dated basaltic flows spanning from 1 to 2 Myrs old that were deposited at the bottom of the former valley (Dautria et al., 2010) are now located at ca 150 m above the current riverbed leading to an average incision rate of 77 ± 10 m.Myr^{-1}, in agreement with karst-inferred incision rates.

Furthermore, preliminary results from canyons on the other side of the Grands Causses (Tarn and Jonte) based on in-situ terrestrial cosmogenic dating suggest similar incision rates (Sartegou et al., 2018b) and confirm a regional base level lowering of the Cévennes and Grands Causses region during the Plio-Quaternary. This is consistent with the similarities of landscapes and lithologies observed both on the Atlantic and Mediterranean watersheds (e.g. Tarn river).

Once the regional pattern of the Plio-Quaternary incision established for the Cévennes-Grands Causses area, the next question is how this river downcutting is related to the regional uplift? First order equilibrium shape and absence of major knick points in the main river profiles preclude the hypothesis of regressive erosion. Hence, back to the three conceptual models presented in part 1 (Fig.2), we can discard, at first order, the models A (Old uplift-recent incision) and B (Old uplift-old incision) because obtain incision rate show recent incision and surface tilting tend to prove a current uplift. Therefore, the incision rate has to be balanced to the first order by the uplift rate. We add that eustatic variations are of too low magnitude (100-120 m) and can't explain such total incision (up to 400m). Furthermore, no obvious evidence of active tectonic is reported for the area raising the question of the processes responsible for this regional uplift. Very few denudation rates are reported for our study area (Schaller et al., 2001; Molliex et al., 2016; Olivetti et al., 2017), and converting canyon incision rates into denudation and erosion rates is not straightforward, especially given the large karst developed in the area. Using a first order erosion/sedimentation profile following the main topography gradient direction we have modelled the erosion-induced isostatic rebound. If this process could create between half and two third of the Plio-Quaternary uplift, a previously existent topography is needed to trigger erosion so it cannot explain neither the onset of the canyon-carving nor the full uplift rates. Other, processes have to be explored such as dynamic topography or thermal anomaly beneath the Massif-Central, the magmatism responsible for the important increase in volcanic activity since ~ 6 Myrs (Michon et Merle, 2001; Nehlig et al., 2003) could play a major role, notably in the initiation of Plio-Quaternary uplift. Further studies should aim to address the problem of uplift onset, giving more clues concerning the stable continental area but owing the data we presently have, discussing such onset is out of the scope of the paper.

5. Conclusion

To the contrary of previous studies that focused on one cave, we have shown that combining karst burial ages and paleomagnetic analysis of clay deposits in several caves over a large elevation range can bring good constraints on incision rates. This multi-cave system approach diminishes the intrinsic limits of the two single methods: low sampling density (and analysis cost) for the TCN ages and difficulty to set the position of paleomagnetic results. Our estimated paleo base level ages are Plio-Quaternary (ca. last 4 Ma) and allow to derive a mean incision rate of 83 $^{+17}/_{-5}$ m.Ma^{-1} for the Cevennes area.

The landscape, and especially the river profiles suggest a first-order equilibrium allowing considering the incision rate as an uplift rate. We propose that related erosional isostatic adjustment is of major importance for the understanding of the southern French Massif-Central landscape evolution and explain a large part of the uplift. However, it is not the only process involved and we hypothesize that is could be especially combined with dynamic topography related to the Massif Central magmatism. Both mechanisms imply an uplift centered on the Massif Central and a radial tilt of the geomorphological surfaces. We have shown using a geomorpholog-

ical analysis that at least south of the Cévennes, several surfaces are tilted toward the SSE. This kind of study had been performed before on large structures (Champagnac et al., 2007) or endokarstic markers (Granger et Stock, 2004) but it is the first time that it is performed at such scale with small markers. Numerical modelling yields the same pattern of SSE dipping, allowing more confidence in the geomorphometric results.
Our multi-disciplinary approach brings the first absolute dating of the Cévennes landscapes and suggests that the present-day morphology is partly inherited from the plio-quaternary erosion-induced isostatic rebound. A strong uplift impact is assumed to be due to magmatic-related dynamic topography that could explain another part of the uplift as well as the onset of such uplift that has afterward been accelerated by the erosion-induced isostatic rebound. These results enlighten the importance of surface processes into lithospheric-scale dynamic and vertical deformations in intra-plate domains.

An analysis at the scale of the Massif Central is now needed before nailing down our interpretations, but such study will more likely highlight the importance of erosion processes to explain uplift of intraplate orogens, and will show that another process is needed for the Massif Central, which will most likely be dynamic topography related to magmatism.

Code availability

Surface analysis was performed using QGIS version 2.18, MAtlab® code and IGN DEM (RGE Alti®) 5m). Modeling was performed using ADELI code (Hassani et Chery, 1996; Chéry et al., 2016). Data for TCN and paleomagnetic analysis are provided in the manuscript itself or in supplementary material.

Author contributions

OM, PV and GC did the sampling. GC and DF performed the TCN analysis. PC and OM did the magnetic measurements and interpretations. OM did the surface identification and analysis. OM, PV and JC performed the numerical model. OM, OV, JFR, GC, PC, JC and DF interpreted and wrote the article.

Competing interests

The authors declare that they have no conflict of interest.

Acknowlegdments

We are grateful to ANSTO for providing facilities for chemical extraction for the TCN analysis. We thanks the reviewers for useful remarks and comments that we think help to increase the level of the paper.

References

Arthaud F. et Laurent P.: Contraintes, déformations et déplacements dans l'avant-pays pyrénéen du Languedoc méditerranéen, Godin. Acta, 8, 142-157, 1995.

Audra P., Camus H. et Rochette P.: Le karst des plateaux de la moyenne vallée de l'Ardèche : datation par paléomagnétisme des phases d'évolution plio-quaternaires (aven de la Combe Rajeau). Bull. Soc. Géol. France, 2001, t. 172. N°1, pp. 121-129, 2001.

Balco, G., Stone, J.O., Lifton, N.A., Dunai, T.J., 2008. A complete and easily accessible means of calculating surface exposure ages or erosion rates from Be-10 and Al-26 measurements. Quat. Geochronol. 3, 174–195. 2008.

Barbarand J., Lucazeau F., Pagel M. Et Séranne M.: Burial and exhumation history of the south-eastern Massif Central (France) constrained by en apatite fission-track thermochronology. *Tectonophysics,* 335, 275-290, 2001.

Barruol G. et Granet M.: A Tertiary astenospheric flow beneath the southern French Massif Central indicated by upper mantle seismic anisotropy and related to the west Mediterranean extension. Earth and Planetary Science Letters 202 (2002) 31-47, 2002.

Brichau S., Respaut J.P. et Monié P.: New age constraints on emplacement of the Cévenol granitoids, South French Massif Central, Int J Earth Sci 97:725–738, doi: 10.1007/s00531-007-0187-x, 2007.

Bruxelles L.: Dépôts et altérites des plateaux du Larzac central : causses de l'Hospitalet et de Campestre (Aveyron, Gard, Hérault) Evolution morphogénétique, conséquences géologiques et implcations pour l'aménagement. Université d'Aix-Marseille I, Université de Provence, UFR Sciences géographiques et de l'aménagement. Thèse, spécialité : Milieux physiques méditerranéens, 2001.

Calais, E., Freed, A. M., Van Arsdale, R., & Stein, S. (2010). Triggering of New Madrid seismicity by late-Pleistocene erosion. Nature, 466(7306), 608–611. http://doi.org/10.1038/nature09258

Calais, E., T. Camelbeeck, S. Stein, M. Liu, and T. J. Craig (2016), A new paradigm for large earthquakes in stable continental plate interiors, Geophys. Res. Lett., 43, doi:10.1002/2016GL070815, 2016.

Calvet M., Gunnell Y., Braucher R., Hez G., Bourlès D., Guillou V., Delmas M. et ASTER team: Cave levels as proxies for measuring post-orogenic uplift : Evidence from cosmogenic dating of alluvium-filled caves in the French Pyrenees. Geomorphology 246 (2015) 617- 633 ; doi : 10.1016/j.geomorph.2015.07.013, 2015.

Camus H.: Vallée et réseaux karstiques de la bordure carbonatée sud-cévenole. Relation avec la surrection, le volcanisme et les paléoclimats. Thèse de doctorat, Université Bordeaux 3, 692 p, 2003.

Champagnac J.D., Molnar P., Anderson R.S., Sue C. et Delacou B.: Quaternary erosion-induced isostatic re-bound in the western Alps. Geology, March 2007 ; v.35 ; no. 3 ; p. 195-198, doi : 10.1130/G23053A.1, 2007.

Champagnac J-D. van der Beek P. Diraison G. et Dauphin S.: Flexural isostatic response of the Alps to in-creased Quaternary erosion recorded by foreland basin remnants, SE France. Terra Nova, Vol 20, No. 3, 213-220, doi : 10.1111/j.1365-3121.2008.00809.x, 2008.

Chéry J., Zoback M.D. et Hassani R.: An integrated mechanical model of the San Andreas Fault in central and northern California. J. Geophys. Res., 106(B10) :22051. 52,61, 2001.

Chéry, J., Genti, M. And Vernant, P. Ice cap melting and low-viscosity crustal root explain the narrow geodetic uplift of the Western Alps.Geophys. Res. Lett.43,1–8 (2016).

Child D.P., Elliott G., Mifsud C., Smith A.M and Fink D., Sample processing for earth science studies at ANTARES. Nuclear Instruments and Methods in Physics Research Section B Beam Interactions with Materials and Atoms 172(1-4):856-860 doi: 10.1016/S0168-583X(00)00198-1, 2000.

Corbel J.: Les phénomènes karstiques dans les Grands Causses. In : Revue de géographie de Lyon, vol. 29, n°4, pp. 287-315, doi : 10.3406/geoca.1954.1990, 1954.

Dautria J.M., Liotard J.M., Bosch D., Alard O.: 160 Ma of sporadic basaltic activity on the Languedoc volcanic line (Southern France): A peculiar cas of lithosphere-astenosphere interplay. Lithos 120 (2010) 202-222, doi: 10.1016/j.lithos.2010.04.009, 2010

Genti M.: Impact des processus de surface sur la déformation actuelle des Pyrénées et des Alpes. Géophysique [physics.geo-ph]. Université de Montpellier, 2015. Français. Thèse, 2016.

Granet M., Wilson M. et Achauer U.: Imaging a mantle plume beneath the French Massif Central. Earth and Planetary Science Letters 136 (1995) 281-296, 1995.

Granger, D. E., Fabel, D. and Palmer, A.N.: Pliocene-Pleistocene incision of the Green River, Kentucky determined from radioactive decay of comogenic 26Al and 10Be in Mammoth Cave sediments. *GSA Bulletin*; July 2001; v. 113; no. 7; p. 825–836

Granger, D. E., Kirchner, J. W., and Finkel, R. C.: Quaternary downcutting rate of the New River, Virginia, measured from differential decay of cosmogenic 26Al and 10Be in cave-deposited alluvium. Geology; Febru-rary 1997 ; v. 25 ; no.2 ; p. 107-110, 1997.

Granger D.E., Gibbon R.J., Kuman K., Clarke R.J., Bruxelles L. and Caffee M.W.: New cosmogenic burial ages for Sterkfontein Member 2 Australopithecus and Member 5 Oldowan, Nature Letter 2015, doi: 10.1038/nature14268, 2015.

Granger D.E. and Muzikar P.F.: Dating sediment burial with in situ-produced cosmogenic nuclides: theory, techniques, and limitations. Earth and Planetary Science Letters 188 (2001) 269-281, 2001.

Granger D.E. and Stock G.M.: Using cave deposits as geologic tiltmeters : Application to postglacial rebound of the Sierra Nevada, California. Geophysical Research Letters, vol. 31, L22501, doi : 10.1029/2004GL021403, 2004.

Zupan Hajna N., Mihevc A., Pruner P. and Bosák P. 2010. Palaeomagnetic research on karst sediments in Slovenia. International Journal of Speleology, 39(2), 47-60. Bologna (Italy). ISSN 0392-6672, 2010.

Haq B.U., Herdenbol J. and Vail P.R.: Mesozoic and cenozoic chronostratigraphy and cycles of sea-level change. Society Economic Paleontologists Mineralogists Special Publication, 42, 71-108, Tulsa, Oklahoma. 1988.

Harmand D., Adamson K., Rixhon G., Jaillet S., Losson B., Devos A., Hez G., Calvet M. and Audra P.: Relationships between fluvial evolution and karstification related to climatic, tectonic and eustatic forcing in temperate regions, Quaternary Science Reviews (2017) 1-19, doi : 10.1016/j.quascirev.2017.02.016, 2017.

Hassani R. and Chery J., Anaelasticity explains topography associated with Basin and Range normal faulting. Geology 24(12):1095. doi: 10.1130/0091-7613(1996)024<1095:AETAWB>2.3.CO;2. 1996.

Hill C.A., 1999.. Sedimentology and Paleomagnetism of sediments, Kartchner caverns, Arizona. Journal of Cave and Karst Studies 61(2) : 79-83, 1999.

Husson E.: Intéraction géodynamique/karstification et modélisation 3D des massifs carbonatés : Implication sur la distribution prévisionnelle de la karstification. Exemple des paléokarsts crétacés à néogènes du Languedoc montpelliérain. Sciences de la Terre. Université Montpellier 2- Sciences et techniques du Languedoc, 236 p, 2014.

Kooi H., Cloetingh S. et Burrus J.: Lithospheric Necking and Regional Isostasy at Extensional Basins 1. Subsidence and Gravity Modeling With an Application to the Gulf of Lions Margin (SE France), Journal of Geophysical Research , vol. 97, no. B12, Pages 17,553- 17,571, november 10, 1992.

Leroux E., Rabineau M., Aslanian D., Granjeon D., Droz L. et Gorini C.: Stratigraphic simulations of the shelf of the Gulf of Lions: testing subsidence rates and sea-level curves during the Pliocene and Quaternary. Terra Nova, Vol 26, No. 3, 230-238, doi: 10.1111/ter.12091, 2014.

Lofi J., Rabineau M., Gorini C., Berne S., Clauzon G;, De Clarens P., Dos Reis A.T., Mountain G.S., Ryan W.B.F, Steckler M.S. et Fouchet C.: Plio-Quaternary prograding clinoform wedges of the western Gulf of Lion continental margin (NW Mediterranean) after the Messinian Salinity Crisis., Marine Geology July 2003; 198 (3-4) : 289-317, doi: 10.1016/S0025-3227(03)00120-8, 2003.

Lucazeau F. and Vasseur G.: Heat flow density data from France and surrounding margins, In: V. Cermak, L. Rybach and E.R. Decker (Editors), Tectonophysics, 164 (1989) 251-258

Manchuel K., Traversa P., Baumont D., Cara M., Nayman E. Et Durouchoux C.: The French seismic CATa-logue (FCAT-17), Bull Earthquake Eng (2018) 16:2227–2251, doi: 10.1007/s10518-017-0236-1, 2018.

Miallier D., Michon L., Evin J., Pilleyre T., Sanzelle S., et Vernet G.: Volcans de la Chaîne des Puys (Massif Central, France) : point sur la chronologie Vasset-Kilian-Pariou-Chopine. Comptes Rendus Géoscience, Elsevier

Michon L. et Merle O.: The evolution of the Massif Central rift: Spatio-temporal distribution of the volcanism. Bulletin de la Society Geologique de France, 2001, t. 172, n°2, pp. 201-211, dog: 102113/172.2.201, 2001.

Miller, K.G., Kominz, M.A., Browning, J.V., Wright, J.D., Mountain, G.S., Katz, M.E.,Sugarman, P.J., Cramer, B.S., Christie-Blick, N., Pekar, S.F.: The Phanerozoic record of global sea-level change. Science 310, 1293–1298, doi : 10.1126/science.1116412, 2005.

Mocochain L.: Les manifestations geodynamiques –Externes et internes- de la crise de salinité messinienne sur une plate-forme carbonatée peri-méditerranéenne : le karst de la basse ardèche (moyenne vallée du rhône ; France). Thèse de doctorat, Université Aix- Marseille I – Université de Provence U.F.R des Sciences géographiques et de l'aménagement Centre Européen de Recherches et d'Enseignement en Géosciences de l'Environnement., 196 p, 2007.

Molliex S., Rabineau M., Leroux E., Bourlès D.L., Authemayou C., Aslanian D., Chauvet F., Civet F. et Jouët G.: Multi-approach quantification of denudation rates in the Gulf of Lion source-to-sink system (SE-France). Earth and Planetary Science Latters 444 (2016) 101-115, doi : 10.1016/j.epsl.2016.03.043, 2016.

Nehlig P., Boivin P., de Goër A., Mergoil J., Prouteau G., Sustrac G. Et Thiéblemont D.: Les volcans du Massif central. Revue BRGM: Géologues, Numéro Spécial: Massif central, 2003.

Nguyen H. N., Vernant P., Mazzotti S., Khazaradze G. et Asensio E.: 3-D GPS velocity field and its implica-tions on the present-day post-orogenic deformation of the Western Alps and Pyrenees. Solid Earth, 7 ; 1349-1363, 2016, doi : 10.5194/se-7-1349-2016, 2016.

Nocquet J.-M. et Calais E.: Crustal velocity field of western Europe from permanent GPS array solutions, 1996-2001. Geophys. J. Int. (2003) 154, 72-88, doi : 10.1046/j.1365-246X.2003.01935.x, 2003.

Nocquet J.-M., Sue C., Walpersdorf A., Tran T., Lenôtre N., Vernant P., Cushing M., Jouanne F., Masson F., Baize S., Chéry J. and Van der Beek P.A., Present-day uplift of the western Alps, Sci. Rep. 6, 28404; doi: 10.1038/srep28404 (2016).

Olivetti V., Godard V., Bellier O. et ASTER team : Cenozoic rejuvenation events of Massif Central topography (France) : Insights from cosmogenic denudation rates and river profiles. Earth and Planetary Science Letters 444 (2016) 179-191, doi : 10.1016/j.epsl.2016.03.049 0012-821X, 2016.

Ouimet, WB, Whipple, KX, Crosby, BT, Johnson, JP, Schildgen, TF. 2008. Epigenetic gorges in fluvial land-scapes. *Earth Surface Processes and Landforms* **33**: 1993– 2009. doi: 10.1002/esp.1650 Epigenetic. 2008.

Rolland Y., Petit C., Saillard M., Braucher R., Bourlès D., Darnault R. Cassol D. Et ASTER Team: Inner gorges incision history: A proxy for deglaciation? Insights from Cosmic Ray Exposure dating (10Be and 36Cl) of river-polished surfaces (Tinée River, SW Alps, France). Earth and Planetary Science Letters, Elsevier, 2017, 457, pp.271 - 281, doi : 10.1016/j.epsl.2016.10.007. <hal-01420882>, 2017.

Rovey II C.W., Balco G., Forir M. Et Kean W.F.: Stratigraphy, paleomagnetism, and cosmogenic-isotope burial ages of fossil-bearing strata within Riverbluff Cave, Greene County, Missouri. Quaternary Research (2017), 1-13, doi : 10.1017/qua.2017.14, 2017.

Saillard M., Petit C., Rolland Y., Braucher R., BOurlès D.L., Zerathe S., Revel M. Et Jourdon A.: Late Quaternary incision rates in the Vésubie catchment area (Southern French Alps) from in situ-produced ^{36}Cl cosmogenic nuclide dating: Tectonic and climatic implications, J. Geophys. Res. Earth Surf., 119, 1121–1135, doi:10.1002/2013JF002985. 2014.

Sanchis E. et Séranne M.: Structural style and tectonic evolution of a polyphase extensional basin of the Gulf of Lion passive margin : the Tertiary Alès basin, southern France. Tectonophysics 322 (2000) 219-242, doi : 10.1016/S0040-1951(00)00097-4, 2000.

Sartégou A.: Évolution morphogénique des Pyrénées orientales: apports des datations de systèmes karstiques étagés par les nucléides cosmogéniques et la RPE. Géomorphologie. Thèse de l'Université de Perpignan. Français <NNT : 2017PERP0044>. <tel-01708921> , 2017.

Sartégou, A., Bourlès, D. L., Blard, P.-H., Braucher, R., Tibari, B., Zimmermann, L., et al. (2018a). Deciphering landscape evolution with karstic networks_ A Pyrenean case study. Quaternary Geochronology, 43, 12–29. http://doi.org/10.1016/j.quageo.2017.09.005

Sartégou A., Mialon A., Thomas S., Giordani A., Lacour Q., Jacquet A., André D., Calmels L., Bourlès D.L., Bruxelles L., Braucher R., Leanni L. Et ASTER team.: When TCN meet high school students: deciphering western Cévennes landscape evolution (Lozère, France) sin g TCN on karstic networks. Poster 4th Nordic Workshop on Cosmogenic Nuclides. 2018b.

Schaller M., von Blanckenburg F., Hovius N. Et Kubik P.W.: Large-scale erosion rates from in situ-produced cosmogenic nuclides in European river sediments. Earth and Planetary Science Letters 188 (2001) 441-458, 2001.

Séranne M., Benedicto A., Labaum P., Truffert C. et Pascal G.: Structural style and evolution of the Gulf of Lion Oligo-Miocene rifting : role of the Pyrenean orogeny. Marine and Petroleum Geology, Vol. 12, No. 8, pp. 809-820, 1995.

Séranne M., Camus H., Lucazeau F., Barbarand J. et Quinif Y.: Surrection et érosion polyphasées de la Bordure cévenole. Un exemple de morphogenèse lente. Bull. Soc. Géol. France, 2002, t. 173, n°2, pp. 97-112, 2002.

Sibuet J.-C., Srivastava S.P. et Spakman W.: Pyrenean orogeny and plate kinematics. Journal of Geophysical Research: Solid Earth, Vol 109, doi: 10.1029/2003JB002514 , 2004.

Spassov S. et Valet J.-P.: Detrial magnetisations from redeposition experiments of different natural sediments. Earth and Planetary Science Letters 351-352 (2012) 147-157, dog: 10.1016/j.epsl.2012.07.016, 2012

Stewart J. and Watts A.B.: Gravity anomalies and spatial variation of flexural rigidity at mountain ranges. Journal of Geophysical research, vol 102, no. B3, Pages 5327-5352, march 10, 1997, doi: 10.1029/96JB03664, 1997.

Stock G.M., Granger D.E., Sasowsky I.D., Anderson R.S. et Finkel R.C.: Coomparison of U-Th, paleomagnetism, and cosmogenic burial methods for dating caves : Implications for landscape evolution studies. Earth en Planetary Science Letters 236 (2005) 388-403, doi : 10.1016/j.epsl.2005.04.024, 2005.

Tarayoun A., Mazzotti S., Gueydan F., Quantitative impact of structural inheritance on present-day deformation and seismicity concentration in intraplate deformation zones, Earth and Planetary Science Letters, Volume 518, 2019, Pages 160-171, ISSN 0012-821X, doi: 10.1016/j.epsl.2019.04.043., 2017.

Tassy A., Mocochain L., Bellier O., Braucher R., Gattacceca J., Bourlès D.: Coupling cosmogenic dating and magnetostratigraphy to constrain the chronological evolution of peri-Mediterranean karsts during the Messinian an the Pliocene: Example of Ardèche Valley, Southern France. Geomorphology, 189 (2013), pp. 81-92, doi: 10.1016/j.geomorph.2013.01.019, 2013.

Tauxe L., Steindorf J.L. et Harris A.: Depositional remanent magnetisation: Toward an improved theatrical and experimental foundation. Earth and Planetary Science Letters 244 (2006) 515-529, doi: 10.1016/J.epsl.2006.02.003, 2006.

Tricart P. : From passive margin to continental collision: A tectonic scenario for the western Alps. American journal of science, Vol. 284, February, 1984, P97-120, 1984.

Vernant, P., Hivert, F., Chéry, J., Steer, P., Cattin, R., & Rigo, A. (2013). Erosion-induced isostatic rebound triggers extension in low convergent mountain ranges. Geology, 41(4), 467–470. http://doi.org/10.1130/G33942.1

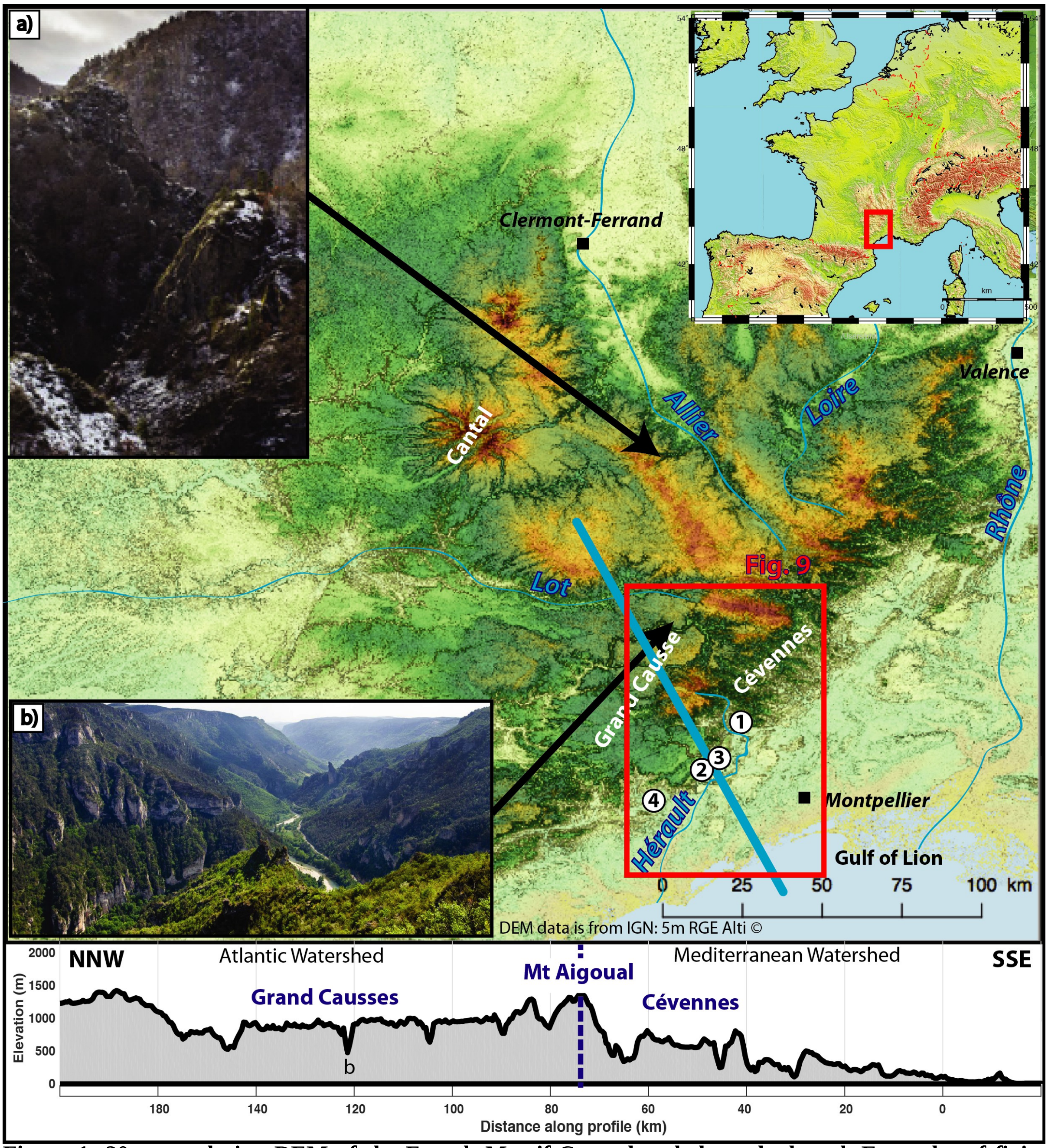

Figure 1: 30 m resolution DEM of the French Massif-Central and slope shadowed. Examples of finite incision typical of the French Massif-Central in a) crystalline area (Seuge Canyon) and b) limestone plateau (Tarn Canyon) Location of the restricted studied area in red box (fig. 9) and numerated site 1) is the Rieutord Canyon (43,958°N; 3.709°E) where TCN measurements have been done, 2) and 3) are the Leicasse Cave System (43,819°N; 3.56°E),and the Garrel Cave system (43,835°N; 3.616°E) respectively, where paleomagnetic analysis have been done and 4) is the Lodève basin (43,669°N; 3.382°E) with dated basaltic flows. Bottom panel is an example of typical topographic profile used for numerical model set up. Note the south-western area with large plateau dissected by canyon, and the rugged area with steep valley called the Cevenne. They are typical regional limestone and crystalline morphology respectively.

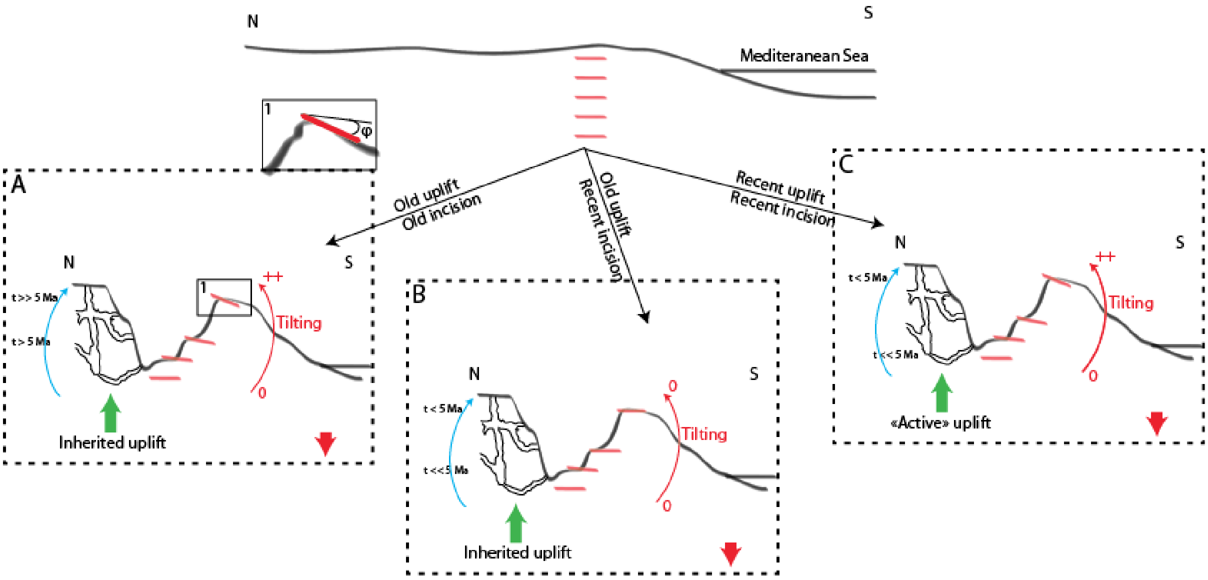

Figure 2: conceptual models for landscape evolution. Top panel is the initial stage (prior to uplift). Each panel represent a possible scenario explaining current morphology: A) Old uplift and old incision, B) Old uplift and recent incision and C) both recent uplift and incision. Blue arrow and associated ages show expected result (or absence of) for burial dating. Red level represents morphological markers that are fossilised when reaching the surface, accumulating afterward (or not) the differential uplift by finite tilting.


Figure 3: Example of quartz cobbles sampled for burial dating. Location: Cuillère Cave

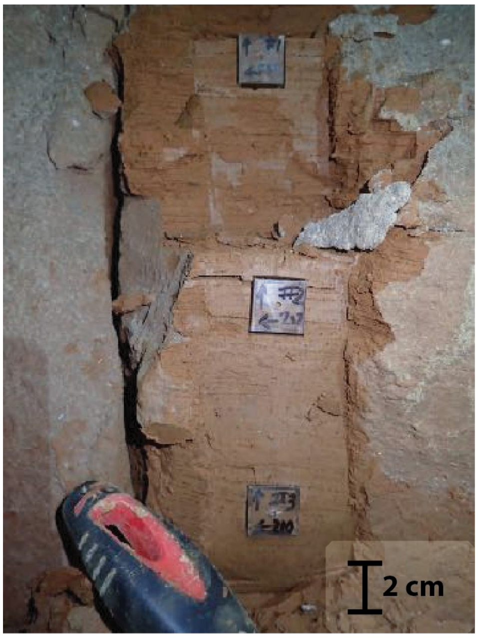

Figure 4: Example of clay sampling for the paleomagnetic study. Location at the entrance shaft (Highest elevation of every samples (~580 m a.s.l.), Leicasse Cave system)

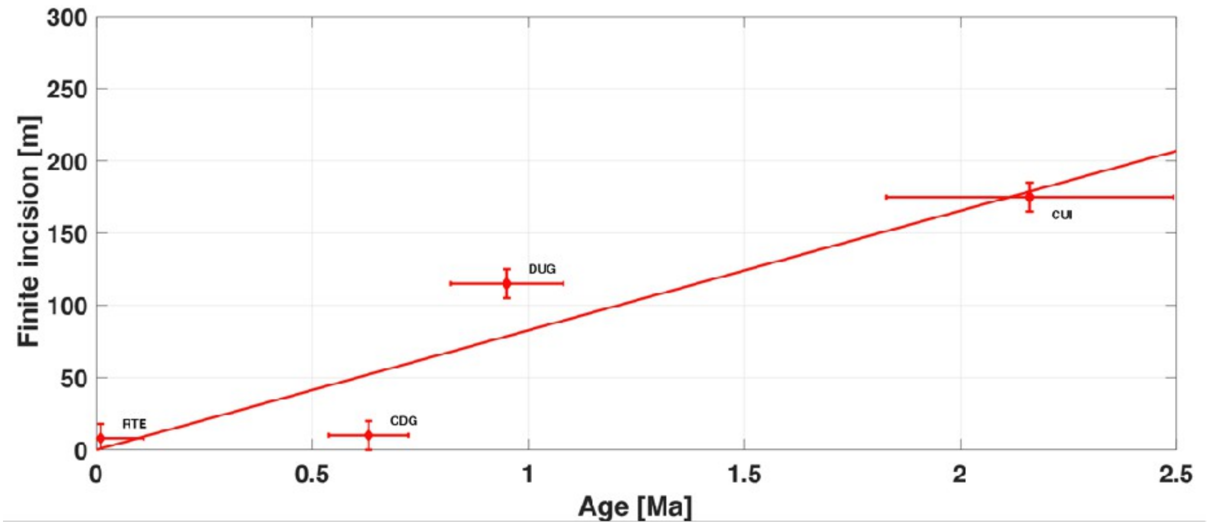

Figure 5: Relation finite incision-burial age for the Rieutord canyon. Finite incision is the elevation of the sampling site relatively to the current riverbed. RTE for Route Cave, CDG for Camp de Guerre Cave, DUG for Dugou Cave and CUI for Cuillère Cave

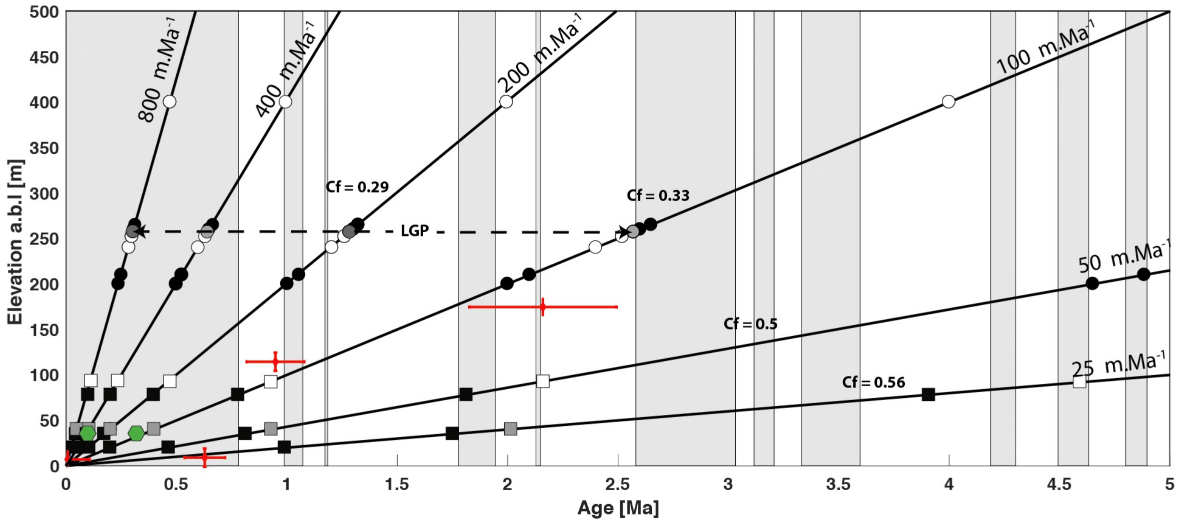

Figure 6. Constraining the incision rate in the Cevennes margin, using paleomagnetic polarities from clay deposits (black, grey and white symbols) and burial ages (red crosses): Circles are from the Le-icasse cave with LGP being *les gours sur pattes profile (see text)*, squares are from the Garrel cave. Black, grey and white symbols correspond to normal, transitional and reverse polarities, respectively. Black linear straight lines define possible incision rates that are supposed stable thought time. (numbers in white rectangles define the Cf values are Ccorrelation factor between the measured paleomagnetic polarities and the predicted paleomagnetic scale (see also Figure 8). Green hexagons show the U/Th ages obtained in the Garrel by Camus (2003).

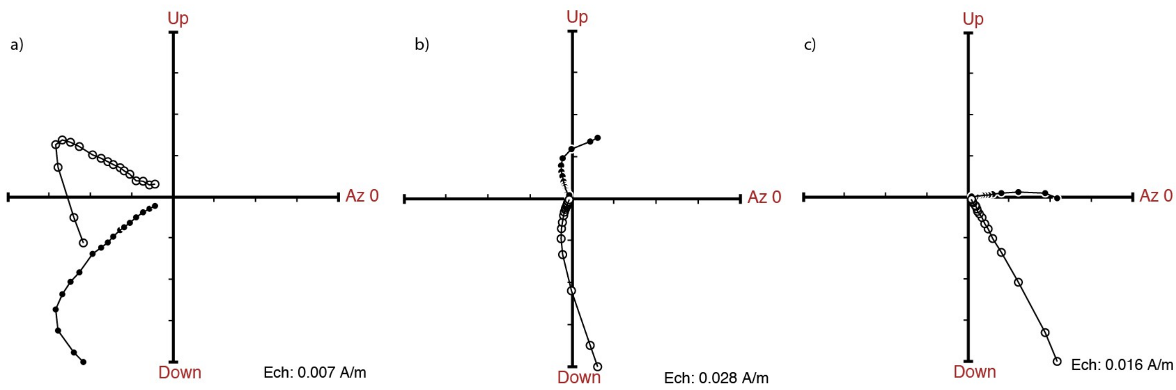

Figure 7: Zijderveld Diagram for three samples from the Gours-sur-Pattes (Leicasse) site. Stratigraphical order is from a) (the older, base of the profile) to c) (the younger, top of the profile.

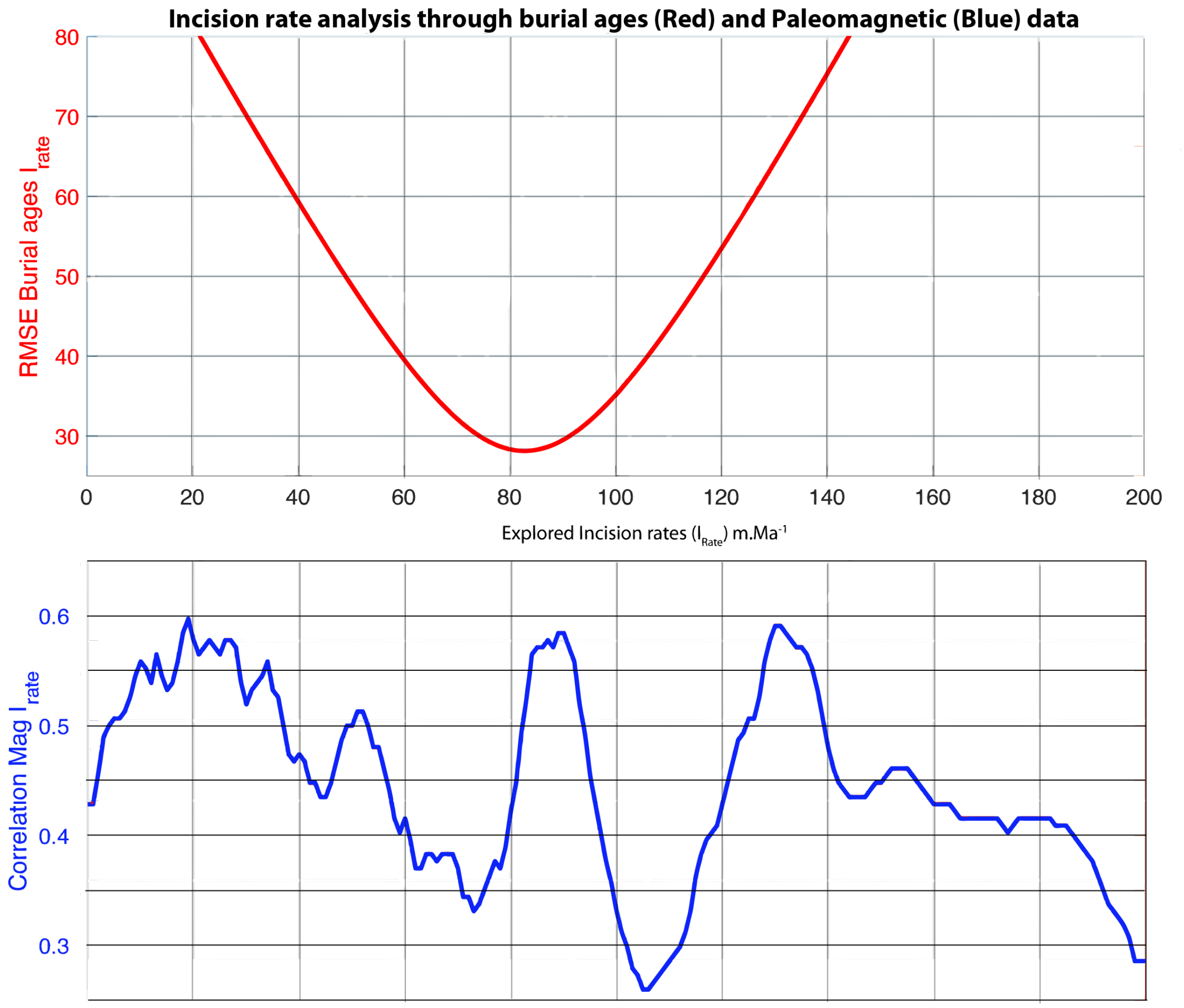

Figure 8: Best incision rate based on paleomagnetic data (blue) and burial ages (red). The blue curve is the normalised smoothed (10 m/Ma sliding window for better visualisation) correlation between theoretical and observed polarities. The highest correlation corresponds to the best incision rates. The red curve is the RMSE for the linear regression through the burial ages data set shown on Fig. 4.

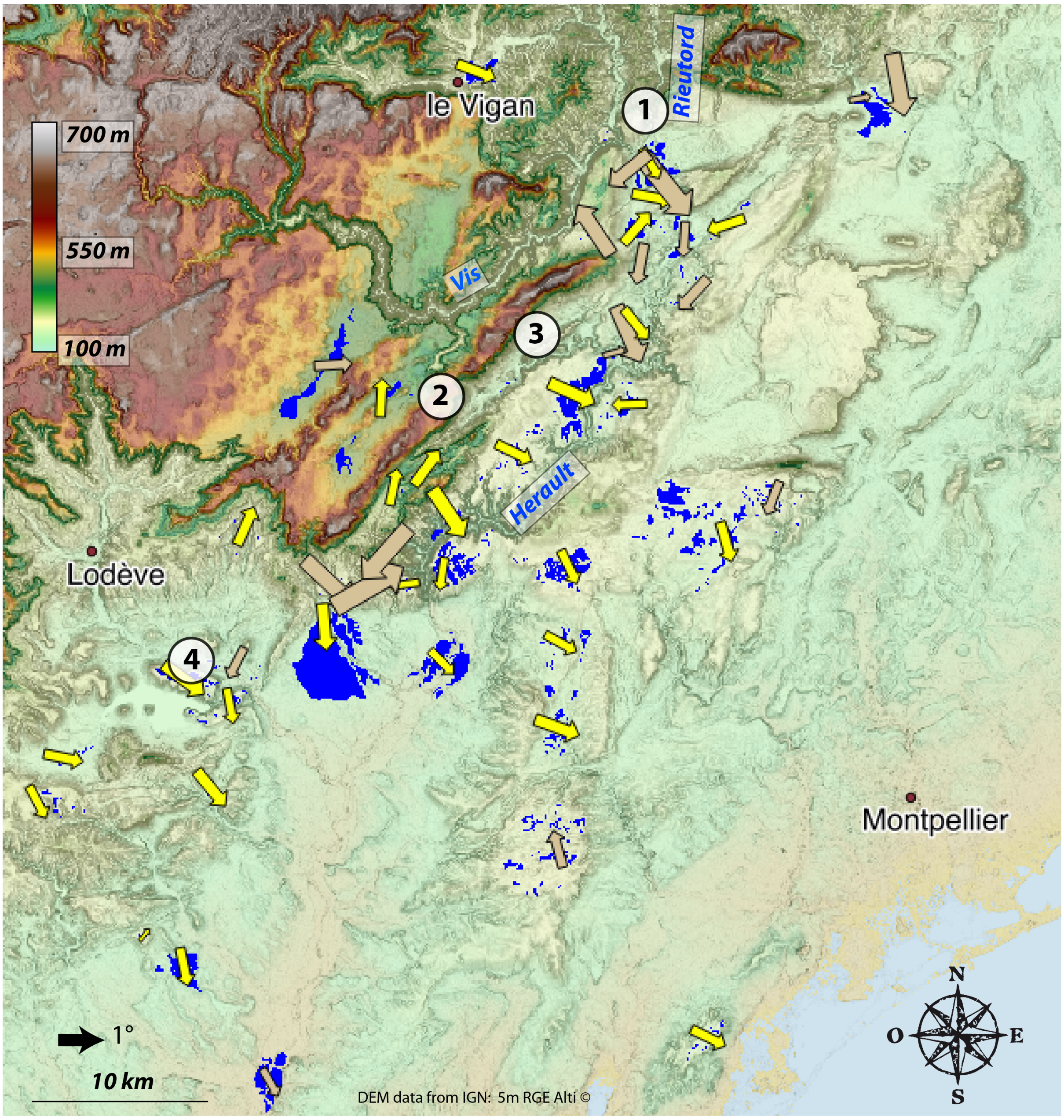

Figure 9: Tilting map of geomorphological benchmark (blue areas). Fond-map is 30 m resolution DEM with slope shadow. Arrows are orientating according to the marker downward dip and sized according to the corrected tilting angle (the bigger, the more the tilting). Yellow and brown arrows are for robust and rejected surfaces respectively. Several arrows are hidden because of their small size and too high proximity with bigger ones. Numerated site 1) is the Rieutord Canyon, 2) is the Leicasse Cave System, 3) is the Garrel Cave system and 4) is the Lodève basin with dated basaltic flows. See Fig. 1 for geographical coordinates.

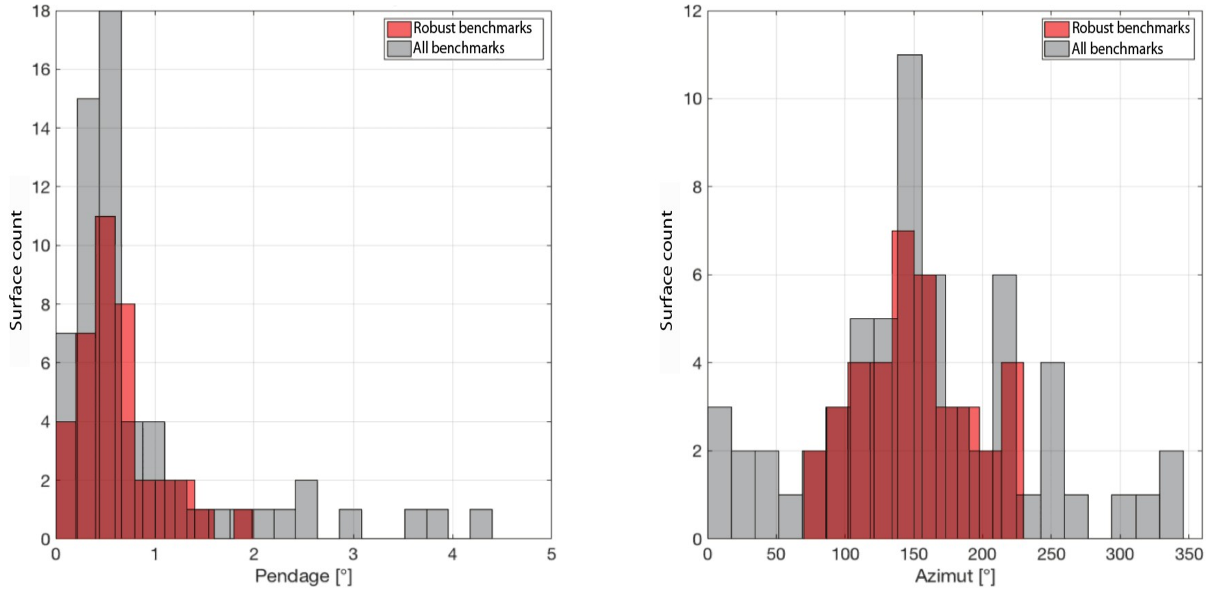

Figure 10: Tilting and azimuth distribution. Left panel is density distribution for surface maximum tilting in degree. Right panel is azimuth of maximum dipping relative to the north. For each histogram, red and grey populations are for robust and primary detected markers.

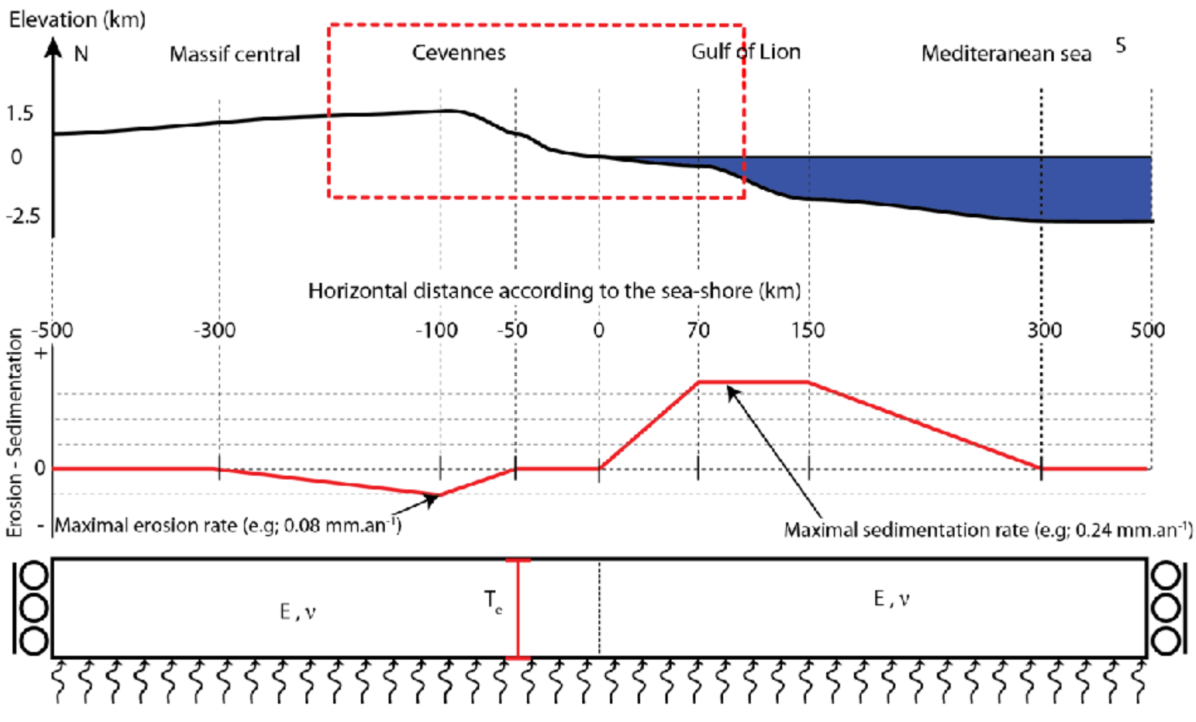

Figure 11: Top panel: schematic topographic profile. The red box delimites the area shown fig. 1 and 9. Middle panel, surface processes profile, negative values are for erosion and positive values for sedimentation. Bottom panel: model set-up with two compartments (one for the Cevennes area and the second on for the gulf of lion). The base of the model is compensated in pressure and the right and left limits are fixed at zero horizontal velocities and free vertical ones. Te is the equivalent elastic thickness (in km), E (Pa) and v are the Young modulus and the Poisson coefficient respectively whom values are independent in each compartment.

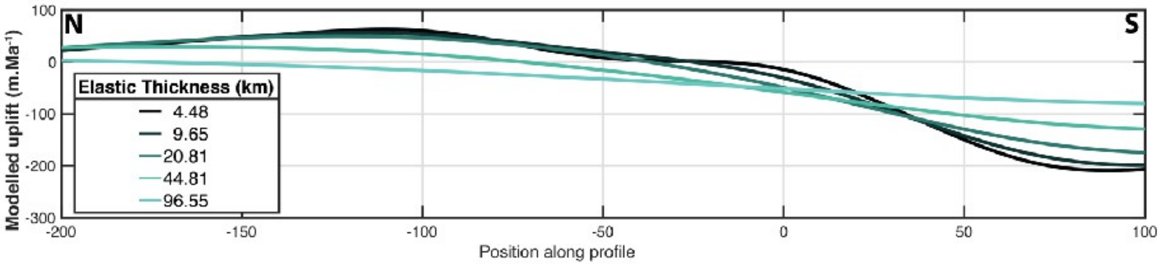

Figure 12: Modelled uplift according to different Te. Most probable Te are between 10 and 30 km.

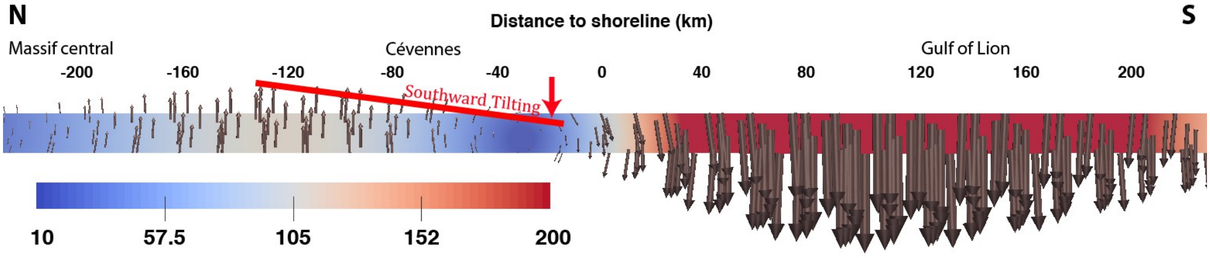

Figure 13: Modelling result for Te= 15km. Erosion-sedimentation rate profile is the same as in fig. 6. Velocity field is shown using arrow for scale and orientation and colour code for value. Black values on top are distance relative to the sea-shore (positive value landward and negative values seaward). Red line represent the southward modelled tilting due to differential uplift.

Cave	Lat	Lon	Elevation	height (a.b.l)	^{10}Be conc (atom/g)	σ ^{10}Be (atom/g)	^{26}Al conc (atom/g)	σ ^{26}Al (atom/g)	26Al/10Be (and error)	Burial age (Ma)	Burial age error (Ma)
RTE	43,960	3,707	175	8	3,54E+04	1,18E+03	2,16E+05	1,47E+04	6,11 +/-0.46	0,20	+0.16/-0.15
CDG	43,955	3,710	185	10	8,87E+04	3,12E+03	4,29E+05	3,28E+04	4,83 +/-0.41	0,67	+0.18/-0.16
DUG	43,957	3,711	245	115	1,27E+04	5,68E+02	5,29E+04	6,36E+03	4,15 +/-0.53	0,99	+0.28/-0.25
CUI	43,959	3,711	354	175	1,70E+04	7,14E+02	3,75E+04	5,28E+03	2,20 +/-0.32	2,28	+0.33/-0.28

Table 1: Samples analytical results and parameters. Cave code are: RTE for the “de la route” Cave, CDG for the “Camp de Guerre” cave, DUG for the “Dugou” Cave and CUI for the “Cuillère” Cave. Main parameters are the geographical coordinate (Lat, Lon in decimals degree), the elevation (a.s.l), the height (a.b.l., computed relatively to the surface river elevation. The concentration (atoms/g quartz) of 10Be and 26Al in collected sand samples are all AMS 10Be/Be and 26Al/Al isotopic ratios corrected for full procedural chemistry blanks and normalised to KN-5-4 and KN -4-2, respectively.The error () is for total analytical error in final average 10Be and 26Al concentrations based on statistical counting error s in final 10Be/Be (26Al/Al) ratios measured by AMS in quadrature with a 1% error in 9Be spike concentration (or a 4% error in 27Al assay in quartz) and a 2% (or 3%) reproducibility error based on repeat of AMS standards. Burial age (minimum) assuming no post-burial

production by muons at given depth (all deeper than 30m) in cave below surface and assuming initial 26Al/10Be ratio is given by the production ratio of 6.75. The burial age error determined by using a +/-1σ range in the measured 26Al/10Be ratio